Available online at www.eccomasproceedia.org
Eccomas Proceedia COMPDYN (2025) 1918-1928

ECCOMAS
Proceedia

COMPDYN 2025
10th ECCOMAS Thematic Conference on
Computational Methods in Structural Dynamics and Earthquake Engineering
M. Papadrakakis, M. Fragiadakis (eds.)
Rhodes Island, Greece, 15-18 June 2025

A FRAMEWORK FOR ASSESSING THE EARTHQUAKE-INDUCED LANDSLIDE RESILIENCE OF A ROAD NETWORK IN TURIN, ITALY

M. Louagie[1], F. Aloschi[2], M. Civera[1], A. Miano[3], B. Chiaia[1] and A. Prota[2]

[1]Department of Structural, Building and Geotechnical Engineering, Polytechnic University of Turin,
Corso Duca degli Abruzzi 24 - 10129 - Turin, Italy
e-mail: marco.civera@polito.it

[2]Department of Structures for Engineering and Architecture, University of Naples "Federico II"
Via Claudio 21 - 80125 - Naples, Italy
e-mail: fabrizio.aloschi@unina.it

[3]Department of Engineering, Telematic University "Pegaso"
Centro Direzionale Isola F2 - 80143 - Naples, Italy

Abstract

Landslides, defined as the downward movement of rock, debris and soil, pose a significant risk to road infrastructure in the Piedmont region, Italy, particularly when triggered by seismic activity and heavy rainfall. This study focuses on assessing the stability and resilience of a rural road network consisting of four primary roads, all connecting the city of Turin, more specifically, the Sassi neighbourhood, with the town of Pino Torinese. Analytical models were integrated into a novel framework for determining the safety factor (FS) and critical acceleration (a_c) for various ground conditions within the identified road network. This method involves the use of GIS data and Digital Elevation Models (DEM) to assess the slope characteristics. Probabilistic seismic hazard analysis (PSHA) models were employed to derive peak ground acceleration (PGA) values, which were then used to calculate Newmark's displacement. Both fully dry and fully saturated conditions were considered to model the boundary conditions of ground stability. Results show that road stability is strongly impacted by soil conditions and slope angles, with stability decreasing as FS approaches the unit value. The highest instability occurs in fully saturated soils due to heavy rainfall, while seismic activity in the studied areas has limited impact. The proposed framework offers valuable insights for designing targeted interventions and assessing road networks' resilience.

Keywords: Landslides; Seismic Risk; Road Network; Seismic Resilience

ISSN:2623-3347
Peer-review under responsibility of the organizing committee of COMPDYN 2025.
doi: 10.7712/120125.12540.24761

1 INTRODUCTION

As climate variability and geological processes increasingly affect human settlements and infrastructure, the need for comprehensive multi-hazard assessments has never been more critical (Gentilucci et al., 2021). In this context, landslides are critical as they represent a geological process in which soil, rock and debris move downward and outward due to gravitational and ground-borne horizontal forces. Seismic activity and heavy rainfall are two major natural forces that can destabilise slopes (Reichenbach et al., 2018) and severely impact road networks. A recent example highlighting the urgency of this issue is the landslide that disrupted the Fréjus tunnel on August 28th, 2023. This tunnel, a key transportation link between Italy and France, was blocked by a landslide in the French Savoy region, causing significant disruptions to mobility and trade.

Along these lines, ensuring resilience in road infrastructure is crucial for maintaining functionality, minimizing recovery time and reducing socio-economic impacts (Wassmer et al., 2024). Resilience not only depends on robust design and disaster mitigation but also on addressing interdependencies within infrastructure networks. Failures in one system, such as power outages, can amplify disruptions in transportation. Strategic planning should integrate both preventive and responsive measures, combining technical solutions with policy frameworks to enhance adaptability and ensure long-term infrastructure stability (Der Sarkissian et al., 2020).

This research assesses the impact of rainfall and earthquakes on slope stability along critical roads in the Piemonte region, Italy. A GIS-based approach was used to analyze recorded landslides in relation to key geotechnical parameters, including the safety factor FS, critical acceleration a_c, and Newmark displacement D_N. Both fully saturated and fully dry soil conditions were considered to capture extreme scenarios. Where direct soil data was unavailable, default values were assigned based on regional averages to maintain consistency. By identifying unstable and marginally stable slopes, this study provides insights that support road management and mitigation strategies. The findings contribute to improving the resilience of transportation networks against natural hazards, ensuring safer and more reliable infrastructure in landslide-prone regions.

2 LANDSLIDE MODELLING

The phenomenon of landslides will always occur due to the influence of destabilizing forces. The occurrence or non-occurrence of such a landslide depends on the magnitude of these forces in relation to the magnitude of the stabilizing forces. The failure of the soil is usually modelled using the Mohr-Coulomb failure criterion, a form of the limit equilibrium method (LEM) (McColl, 2022; Po Wong et al., 2022). As shown in Figure 1, these destabilizing forces include gravity. A certain safety factor can thus be assigned to each particle of land within a slope by simply determining the ratio of the stabilizing, resisting forces to the destabilizing, driving forces (McColl, 2022). Apart from the shear stresses caused by gravity, which are always present in the soil, additional temporary driving stresses, known as triggers, can exceed the soil's resistance to movement. These triggers can result from various factors, such as heavy rainfall or seismic activity.

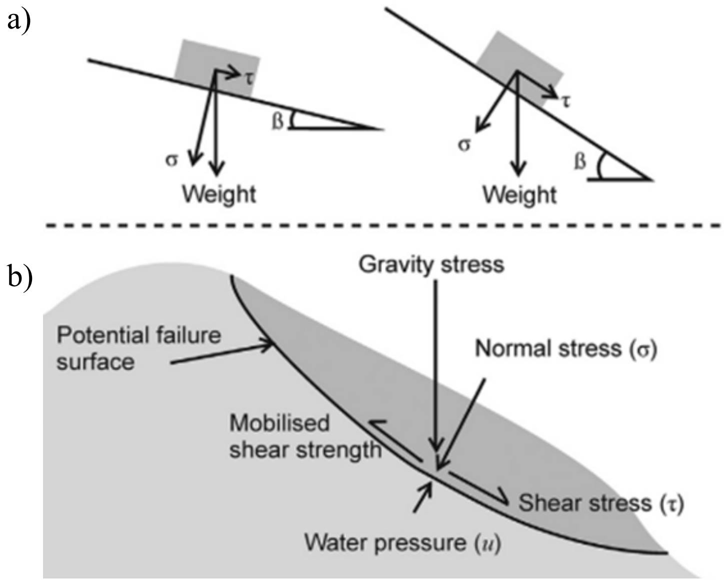

Figure 1: a) Influence of the slope angle; b) stresses along a potential failure surface (McColl, 2022).

The two triggers discussed in this paper are earthquake-induced landslides (EQIL) and rainfall-induced landslides (RIL). EQILs occur when a slope that is initially marginally stable becomes unstable due to seismic activity (Popescu, 2002; Sassa et al., 1996). This activity generates both vertical and horizontal ground shaking, with horizontal acceleration acting as a driving force that destabilises the ground. This paper examines peak ground acceleration (PGA), which measures the intensity of horizontal acceleration caused by an earthquake. If PGA exceeds a slope-specific threshold, the trigger is considered strong enough to cause instability and failure, resulting in an EQIL (Gutiérrez & Gutiérrez, 2016; Sassa et al., 1996). RILs, on the other hand, occur when heavy or prolonged rainfall saturates the soil, reducing its stability and increasing pore water pressure. If this process weakens the slope beyond its resistance capacity, failure occurs, leading to a RIL (Gutiérrez & Gutiérrez, 2016).

To apply the method discussed later, several assumptions and simplifications are made. These are necessary due to limited data availability, either because certain on-site tests are impractical or because detailed information is unavailable. Thus, we apply the rigid-block model, through the so-called limit equilibrium method (LEM) under the assumption of a planar sliding surface, simplifying the calculation of the safety factor. This allows for the use of linear equations based on translational equilibrium, applicable to localised failures, namely, block failure, or unstable slope sections, namely, infinite slope model (Christian & Baecher, 2015). However, due to uncertainties in the depth and extent of sliding surfaces, the infinite slope assumption is deemed unsuitable, and a rigid-block model is adopted instead. Such a rigid-block model better aligns with the available data and site conditions while enabling the use of Newmark's displacement calculations. Several key assumptions support this approach: slope deformation is treated as a two-dimensional problem, the safety factor is assumed uniform across the slip surface, and material behaviour follows a rigid, perfectly plastic model, where failure occurs without strength changes. Additionally, the sliding surface is predefined with a fixed planar or curvilinear shape.

Landslide susceptibility is assessed using key geotechnical parameters, such as effective internal friction angle, effective cohesion, and volumetric weight, which are determined from soil samples. These values are recorded in a project GIS and assigned to nearby landslides previously documented in the study area. Since high-density sampling across the entire area is not feasible, a GIS-based spatial analysis is used to estimate parameters in unsampled locations. Buffer zones of 500 meters are created around each sample point, assigning landslides within these zones the parameters of the nearest sample. Landslides outside these zones are assigned the average values of all available samples. If a sample lacks certain parameters, missing values are supplemented with these averages. This method maintains consistency and enhances the reliability of the assessment.

Another key assumption in this study is the soil thickness perpendicular to the failure surface, a crucial but uncertain parameter used in the calculation of the safety factor explained later. Due to soil heterogeneity, the depth of the critical slip plane cannot be determined solely from empirical data. Instead, predictive models estimate the failure depth, where soil resistance is lowest and failure most likely, while stability increases at other depths. Given the limitations of in-situ testing and modelling, a uniform soil thickness of 3 meters is assumed, based on established methods in geotechnical investigations (Jing et al., 2023; Wu, 2015). This depth is often associated with layer separations, which may serve as potential settlement surfaces. While this assumption is in good agreement in some areas, it introduces uncertainty in others. A greater thickness reduces cohesive strength and lowers the safety factor, while a smaller thickness increases resistive stresses and improves stability.

The final assumption in this study concerns the parameter m, i.e., the ratio of saturated soil thickness to the total soil thickness. This factor is influenced by precipitation intensity and is difficult to determine accurately. Ideally, m can be derived from in-situ testing or probabilistic analysis, but due to limited data, two simplified scenarios are used to represent extreme soil saturation ratios. The best scenario assumes completely dry soil with $m = 0$, where no saturation occurs and, therefore, the soil maintains its maximum shear strength. This occurs after long periods of drought or at extremely low groundwater levels. The worst-case scenario assumes fully saturated soil with $m = 1$, in which water saturates the entire soil layer and significantly reduces the strength of the soil. Although full saturation is rare, it becomes more likely during periods of heavy rainfall. We acknowledge that soil moisture fluctuates due to seasonal and environmental factors, but these variations are simplified to two fixed values for the sake of simplicity. In addition, this approach only considers soil saturation and not increased groundwater pressure, which can further reduce slope stability (Zong et al., 2024).

3 SEISMIC HAZARD SCENARIO AND METHODOLOGY

This paper proposes an analytical method to determine the hazard of a landslide and allows determining the safety factor and the impact of seismic activity on a slope. This method not only determines the probability of occurrence but also provides a framework to go beyond hazard assessment and incorporate risk assessment. While hazard assessment focuses solely on estimating the likelihood of a specific event at a given location, this approach allows for a more comprehensive analysis by also considering its potential consequences. In this context, road networks are highly vulnerable to a multitude of natural hazards, such as earthquakes, heavy rainfall, and floods, which cause landslides and severe disruptions, economic losses, and safety risks. We developed a method for analytically assessing landslide hazards, considering both EQILs and RILs. With probabilistic seismic hazard analysis (PSHA), digital elevation models (DEM) and geological data available, both the safety factor (FS) and Newmark's displacement D_N can be determined. The following procedure is used based on the flowchart presented in Figure 2.

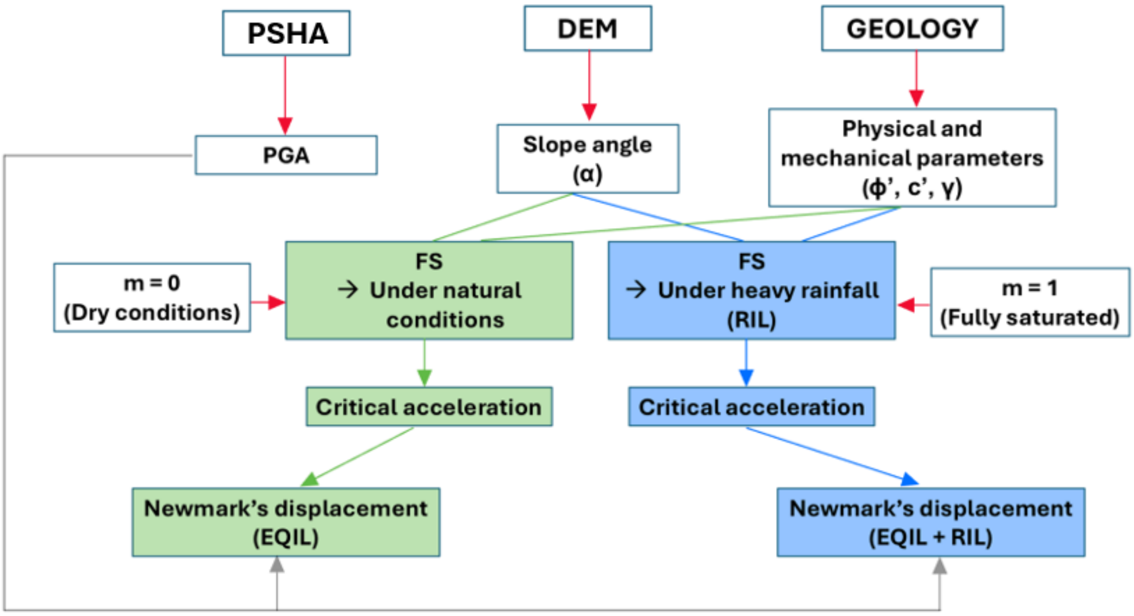

Figure 2: Flowchart of the methodology used to compute EQIL and RIL.

Probabilistic Seismic Hazard Analysis (PSHA) is used to estimate Peak Ground Acceleration (PGA) by evaluating the probability of different levels of earthquake-induced ground motion at a given location over a specific time period. This method integrates seismic source zones, earthquake magnitude distributions and Ground Motion Prediction Equations (GMPEs) through a logic tree approach (Iervolino et al., 2023). Each branch in the logic tree represents a different seismic scenario, weighted based on expert opinions and historical data (Anbazhagan et al., 2019).

As already hinted before, the soil saturation parameter m is here defined as the ratio of saturated soil thickness to the total soil thickness. This is a key parameter influencing slope stability. Due to the absence of direct in-situ measurements, this study adopts a simplified approach by considering two extreme scenarios: dry conditions, m = 0, and fully saturated conditions, m = 1. In the dry scenario, the soil retains its maximum shear strength, leading to a higher safety factor. Conversely, in the fully saturated scenario, increased pore water pressure reduces shear strength, lowering the FS and making slope failure more likely. The slope angle α is critical in landslide susceptibility, as steeper slopes are more prone to failure due to increased gravitational forces. In this study, the slope angle is derived from a digital elevation model (DEM). The DEM provides topographic data, being the height of two points of interest and the horizontal distance between them, allowing for the calculation of local slope gradients across the study area.

The safety factor (FS) is calculated to assess slope stability using Eq. (1). An FS > 1 indicates a marginally stable slope, while an FS < 1 suggests potential failure. This study employs the rigid-block model, which aligns with the Newmark displacement method for seismic analysis. According to Jibson et al. (Jibson et al., 2000), the FS is determined as follows,

$$FS = \frac{c'}{\gamma \cdot t \cdot sen\alpha} + \frac{tan\varphi'}{tan\alpha} - \frac{m \cdot \gamma_w \cdot tan\varphi'}{\gamma \cdot tan\alpha} \tag{1}$$

where c' is effective cohesion, γ is the unit weight of the soil, t is the soil thickness perpendicular to the failure surface, α is the slope angle, ϕ' is the effective internal friction angle, m is the saturation ratio and γ_w is the unit weight of water. The critical acceleration, a_c, represents the minimum horizontal acceleration required to initiate slope failure. It is a key parameter in assessing seismic slope stability, as it defines the threshold at which driving forces exceed resisting forces. A positive a_c indicates a stable slope, whereas a negative a_c suggests inherent instability. The critical acceleration is calculated as follows,

$$a_c = (FS - 1)g \cdot sin\alpha \tag{2}$$

where FS is the safety factor, g is the gravitational acceleration, and α is the slope angle. To finally assess the Newmark's displacement, D_N, which estimates the permanent movement of a slope during seismic loading, we employ the approach proposed by Niño et al. (Niño et al., 2014). This value does not necessarily provide the actual effective displacement of the soil but rather serves as an estimate of the potential movement of the slope under loading conditions, and is assed as follows,

$$\ln(D_N) = -1{,}708 + \ln\left[\left(1 - \frac{a_c}{a_{max}}\right)^{2{,}10}\left(\frac{a_c}{a_{max}}\right)^{-1{,}783}\right] \pm 1{,}04 \tag{3}$$

where a_c is the critical acceleration, and a_{max} is the peak ground acceleration. D_N is only meaningful if $a_c < a_{max}$, ensuring that seismic forces exceed the slope's resistance threshold.

4 APPLICATION TO THE TURIN RURAL ROAD NETWORK

The study area is located in Piedmont, Italy, focusing on the road network between Sassi and Pino Torinese near Turin. This region was selected due to its strategic importance and high landslide susceptibility. The analysis considers four key paths: these are referred to here as Panoramica, Pino Nuovo (SS10), Pino Vecchio, and Eremo. Triggered by rainfall and seismic activity, the landslides pose risks to infrastructure and mobility. ISPRA, Istituto Superiore per la Protezione e la Ricerca Ambientale, provides a useful web platform as a database for landslides and floods, as shown in Figure 3. Each red dot represents a registered landslide that occurred in the past. The study area is located in the landslide-dense region just south of Turin's city centre.

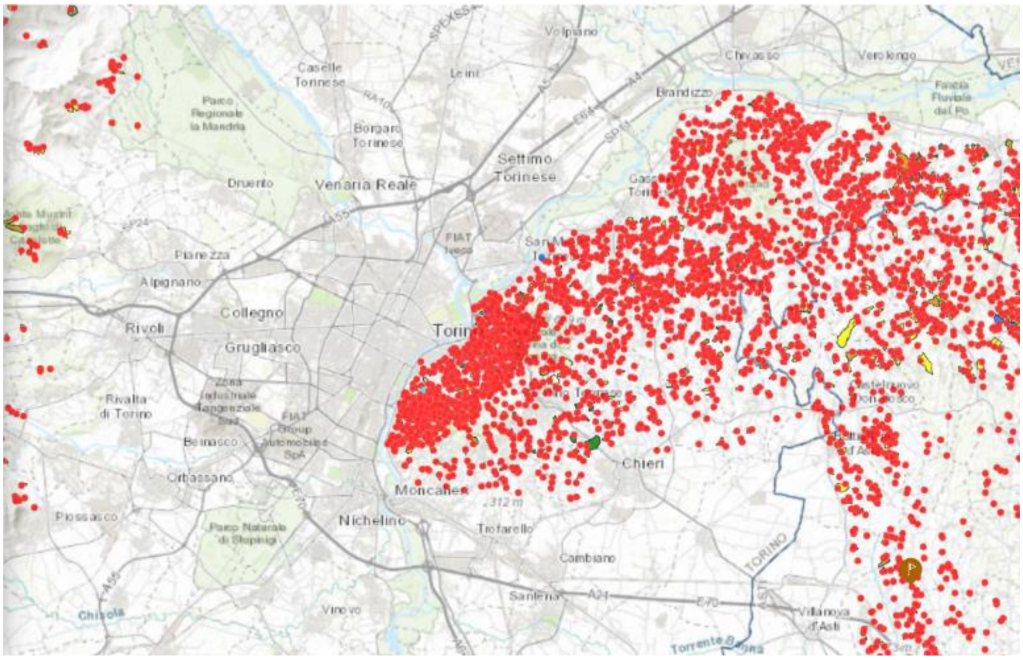

Figure 3: Visualisation of recent landslides in the area of interest extracted from the Italian web platform IdroGEO on landslides and floods; landslides are marked by red dots.

The four roads connecting Pino Torinese and Sassi are integrated into a project GIS, along with all landslides recorded by ISPRA that intersect or are in proximity to these roads, shown in Figure 4. The region is characterised by a relatively low peak ground acceleration (PGA), uniformly assumed to be 0.050g. However, it experiences frequent and intense rainfall, which is likely the primary cause of slope failures.

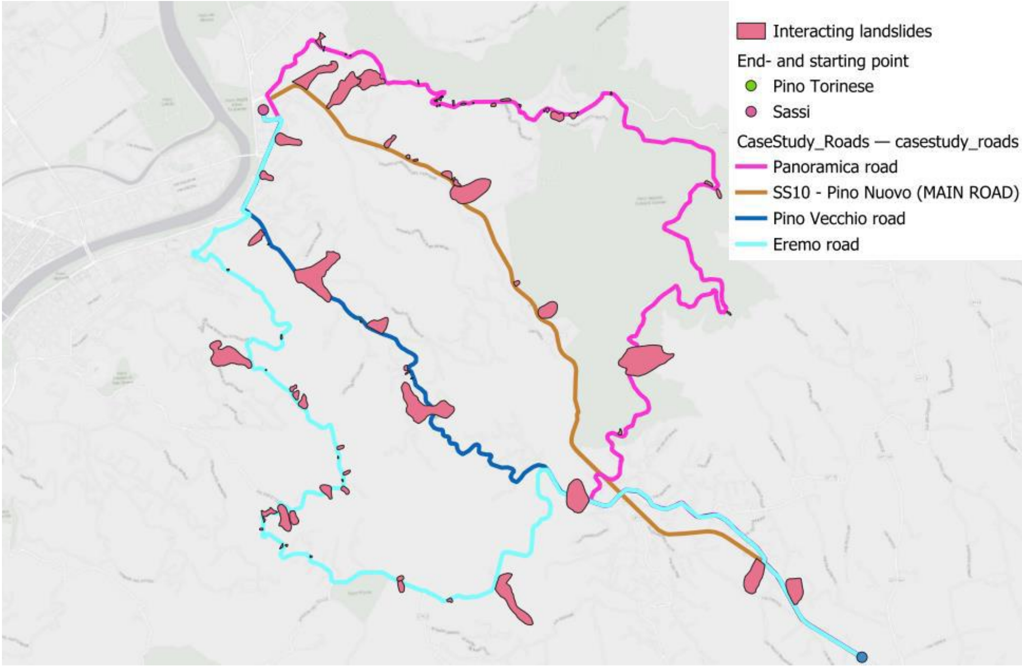

Figure 4: The four chosen paths in the study area.

The slope angle was determined using Google Earth, while soil parameters were obtained from samples and perforations conducted by ARPA (Agenzia Regionale per la Protezione Ambientale), a geotechnical database for the Piedmont region. These values were added to the project GIS. To assign default values, ARPA samples were also numbered and included in the GIS with a 500 m buffer, as shown in Figure 5.

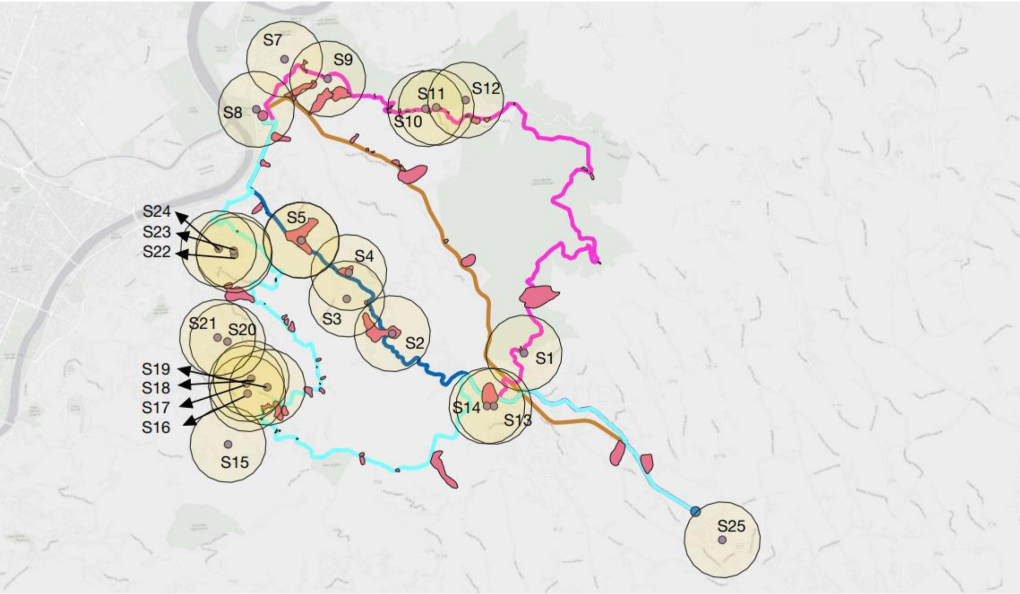

Figure 5: project GIS with buffered samples (radius 500m).

Landslides outside these buffers were assigned default values, as listed in Table 1.

Table 1: Default values of the soil parameters.

Soil parameter	Notation	Default value
Friction angle	ϕ’	25.64°
Cohesion	c’	20.70 kPa
Volumetric weight of the soil	γ	19.19 kN/m³

5 RESULTS

All the recorded landslides shown in Figure 4 were used in this application. Firstly, the safety factor (FS) was calculated under the worst-case scenario of full saturation, followed by a dry condition where the saturation ratio was set to zero. For each landslide, the critical acceleration a_c and Newmark's displacement D_N were also determined. Figure 6 a) and b) depict the landslides in fully saturated and dry conditions, respectively.

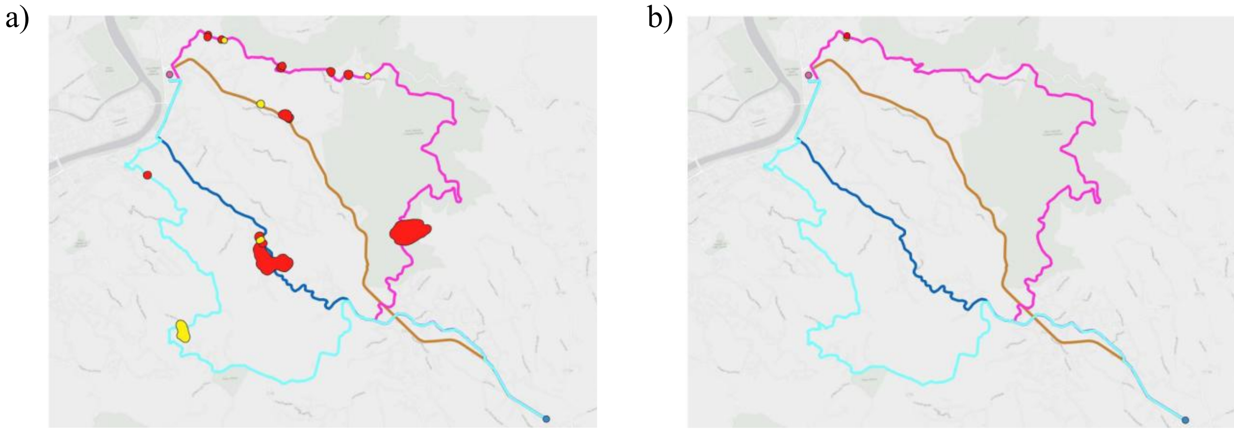

Figure 6: a) Landslides under fully saturated conditions. RILs are depicted in red while EQIL + RIL in yellow. b) Landslides in dry conditions. Natural dry conditions (red) and EQIL (yellow).

Figure 6 a) shows that all the roads studied are prone to landslides, which can be triggered by RILs, or a combination of rainfall and seismic activity. The Panoramica road, located at the top of the figure, is the most affected, with eleven potential landslide locations that could block the road if triggered. In contrast, Figure 6 b) indicates that only the Panoramica road is vulnerable under natural dry conditions or when seismic activity occurs, highlighting its higher susceptibility compared to the other roads in the area.

To further quantify these findings, Table 2 presents the results for Panoramica Road under both extreme conditions. The same colour-coding as in Figure 6 is applied: landslides with FS < 1 and thus negative a_c are marked in red, as they are inherently unstable. For these cases, Newmark's displacement cannot be determined, as it would lead to an undefined result in Eq. (3). Their failure is, therefore, not due to seismic activity. Conversely, landslides where seismic activity contributes to failure are highlighted in yellow. In these cases, FS > 1, and a nonzero Newmark's displacement (D_N) is observed. Under fully saturated conditions (m = 1), the red-marked landslides are classified as RILs, while the yellow-marked ones represent a combination of RIL and EQIL. LP2 and LP5, respectively, from Table 2 are an example of this. Under fully dry conditions, the yellow landslides are considered EQILs (LP2), while the red ones indicate locations that are already unstable under natural dry conditions, without additional external triggers (LP3). This contradicts reality and is further explained in the following section.

Table 2: Safety factor (FS), critical acceleration (a_c), and Newmark's displacement (D_N) assessed for the landslides relevant to Panoramica road, in both dry (m = 0) and fully saturated soil conditions (m = 1); the landslides highlighted in red are the RILs, while the yellow highlights the EQILs.

		m = 1			**m = 0**		
ID	α [°]	FS [/]	a_c [g]	D_N [m]	FS [/]	a_c [g]	D_N [m]
LP1	18.43	1.40	0.13		2.01	0.32	
LP2	34.93	0.73	-	-	1.02	0.01	2.73
LP3	38.07	0.66	-	-	0.92	-	-
LP4	38.82	0.89	-	-	1.22	0.14	
LP5	33.69	1.02	0.01	1.03	1.42	0.23	
LP6	18.65	1.85	0.27		2.64	0.52	
LP7	16.70	2.03	0.30		2.85	0.53	
LP8	38.96	0.88	-	-	1.19	0.12	
LP9	34.80	0.98	-	-	1.35	0.20	
LP10	34.80	0.98	-	-	1.35	0.20	
LP11	25.63	1.34	0.15		1.87	0.38	
LP12	19.92	1.70	0.24		2.38	0.47	
LP13	27.15	1.26	0.12		1.76	0.35	
LP14	26.34	1.30	0.13		1.82	0.36	
LP15	27.76	1.23	0.11		1.72	0.34	
LP16	23.96	1.43	0.17		2.01	0.41	
LP17	28.72	1.19	0.09		1.66	0.32	
LP18	24.08	1.42	0.17		2.00	0.41	
LP19	23.87	1.44	0.18		2.02	0.41	
LP20	38.77	0.88	-	-	1.20	0.13	
LP21	18.97	1.77	0.25		2.44	0.47	
LP22	38.32	0.86	-	-	1.16	0.10	
LP23	25.05	1.33	0.14		1.83	0.35	
LP24	22.85	1.46	0.18		2.01	0.39	
LP25	31.66	1.05	0.03	0.12	1.43	0.22	
LP26	23.47	1.44	0.18		2.01	0.40	
LP27	22.65	1.50	0.19		2.08	0.42	
LP28	25.55	1.32	0.14		1.84	0.36	
LP29	25.02	1.35	0.15		1.88	0.37	
LP30	34.32	0.98	-	-	1.34	0.19	
LP31	24.24	1.56	0.23		2.11	0.46	
LP32	6.00	5.67	0.49		8.00	0.73	
LP33	9.50	3.58	0.43		5.05	0.67	

6 CONCLUSIONS

In this study, we developed a framework for assessing the impact of earthquakes and heavy rainfall on landslide susceptibility along a road network in the Piemonte region, Italy. The findings indicate that slope instability is primarily driven by a combination of steep terrain, unfavourable soil properties and high saturation levels due to intense rainfall, rather than seismic activity.

A key methodological choice was the use of default soil parameters for areas lacking direct sample data. These default values, derived from the average of available samples, ensured a consistent approach. However, an alternative could involve assigning the most critical values, i.e., lowest friction angle, cohesion and unit weight, which would provide a more conservative assessment.

The results reveal several cases where the safety factor (FS) is below 1, which theoretically indicates slope failure. In reality, no additional landslides have occurred at these locations since the previously recorded events, suggesting that the actual safety factor must be greater than 1. Examples of such cases on Panoramica Road include LP2, LP3, LP4, and others, as shown in Table 2. This discrepancy may be attributed to the use of default soil values, which could be more conservative than real conditions, or to the assumption of fully saturated soil, which is unlikely to be consistently present in practice. LP3 in completely dry conditions demonstrates that differences between the calculated FS values and reality cannot be solely attributed to soil saturation. Therefore, other factors must also play a significant role. The assumption of a uniform soil thickness of 3 meters above the failure surface across all locations introduces uncertainty, as the actual depth of this critical surface may vary significantly. A greater thickness would typically result in a lower FS, while a thinner layer could increase stability. Moreover, the rigid-block model used for stability calculations assumes a planar sliding surface, which may not accurately represent the complexity of real slope failures. This simplification could lead to either an overestimation or underestimation of stability, depending on the actual geometry of the failure surface. These aspects highlight the inherent limitations of analytical modelling and suggest that refining input data, incorporating more detailed field measurements, and considering more advanced modelling techniques could improve the accuracy of FS predictions.

The results provide geotechnical, structural, and transportation engineers with valuable insights into road infrastructure resilience, supporting targeted mitigation strategies. The calculation of critical acceleration further refines the assessment of slope sensitivity to external triggers, such as earthquakes. Future research could incorporate Monte Carlo simulations to evaluate stochastic resilience indices. The developed database and proposed methodology offer a solid foundation for further resilience assessments.

ACKNOWLEDGMENTS

The authors acknowledge the project PE3 RETURN, Spoke: TS2 - MULTI-RISK RE-SILIENCE OF CRITICAL INFRASTRUCTURES. MUR project code: PE00000005 and the project CN-MOST within the European Union Next-Generation EU (PNRR) – MISSIONE 4 COMPONENTE 2, INVESTIMENTO 1.4 – D.D. 1033 17/06/2022, CN00000023). The authors also acknowledge the project MOST – Sustainable Mobility National Research Center and received funding from the European Union Next-Generation EU (PIANO NAZIONALE DI RIPRESA E RESILIENZA (PNRR) – MISSIONE 4 COMPONENTE 2, INVESTIMENTO 1.4 – D.D. 1033 17/06/2022, CN00000023). Finally, the authors would like to thank Prof. Dr. Ir. P. Van den Broeck from KU Leuven for his support and Dr. Giulia la Porta from Politecnico di Torino for the insightful discussions.

REFERENCES

Anbazhagan, P., Bajaj, K., Matharu, K., Moustafa, S. S. R., & Al-Arifi, N. S. N. (2019). Probabilistic seismic hazard analysis using the logic tree approach – Patna district (India). *Natural Hazards and Earth System Sciences*, *19*(10), 2097–2115. https://doi.org/10.5194/nhess-19-2097-2019

Christian, J. T., & Baecher, G. B. (2015). D. W. Taylor and the Foundations of Modern Soil Mechanics. *Journal of Geotechnical and Geoenvironmental Engineering*, *141*(2). https://doi.org/10.1061/(ASCE)GT.1943-5606.0001249

Der Sarkissian, R., Abdallah, C., Zaninetti, J.-M., & Najem, S. (2020). Modelling intra-dependencies to assess road network resilience to natural hazards. *Natural Hazards*, *103*(1), 121–137. https://doi.org/10.1007/s11069-020-03962-5

Gentilucci, M., Materazzi, M., & Pambianchi, G. (2021). Statistical Analysis of Landslide Susceptibility, Macerata Province (Central Italy). *Hydrology*, *8*(1), 5. https://doi.org/10.3390/hydrology8010005

Gutiérrez, F., & Gutiérrez, M. (2016). Slope Movements. In *Landforms of the Earth* (pp. 127–154). Springer International Publishing. https://doi.org/10.1007/978-3-319-26947-4_8

Iervolino, I., Chioccarelli, E., & Cito, P. (2023). Testing three seismic hazard models for Italy via multi-site observations. *PLOS ONE*, *18*(4), e0284909. https://doi.org/10.1371/journal.pone.0284909

Jibson, R. W., Harp, E. L., & Michael, J. A. (2000). A method for producing digital probabilistic seismic landslide hazard maps. *Engineering Geology*, *58*(3–4), 271–289. https://doi.org/10.1016/S0013-7952(00)00039-9

Jing, J., Wu, Z., Chu, C., Ding, W., & Ma, W. (2023). Prediction of landslide hazards induced by potential earthquake in Litang County, Sichuan, China. *Natural Hazards*, *118*(2), 1301–1314. https://doi.org/10.1007/s11069-023-06050-6

McColl, S. T. (2022). Landslide causes and triggers. In *Landslide Hazards, Risks, and Disasters* (pp. 13–41). Elsevier. https://doi.org/10.1016/B978-0-12-818464-6.00011-1

Niño, M., Jaimes, M. A., & Reinoso, E. (2014). Seismic-event-based methodology to obtain earthquake-induced translational landslide regional hazard maps. *Natural Hazards*, *73*(3), 1697–1713. https://doi.org/10.1007/s11069-014-1163-y

Po Wong, K., Zhang, Y., & Cheng, Q. (2022). Introductory Chapter: Landslides. In *Landslides*. IntechOpen. https://doi.org/10.5772/intechopen.99301

Popescu, M. E. (2002). *Landslide causal factors and landslide remediatial options*.

Reichenbach, P., Rossi, M., Malamud, B. D., Mihir, M., & Guzzetti, F. (2018). A review of statistically-based landslide susceptibility models. *Earth-Science Reviews*, *180*, 60–91. https://doi.org/10.1016/j.earscirev.2018.03.001

Sassa, K., Fukuoka, H., Scarascia-Mugnozza, G., & Evans, S. (1996). Earthquake-induced-landslides : distribution, motion and mechanisms. *SOILS AND FOUNDATIONS*, *36*(Special), 53–64. https://doi.org/10.3208/sandf.36.Special_53

Wassmer, J., Merz, B., & Marwan, N. (2024). Resilience of transportation infrastructure networks to road failures. *Chaos: An Interdisciplinary Journal of Nonlinear Science*, *34*(1). https://doi.org/10.1063/5.0165839

Wu, X. Z. (2015). Development of fragility functions for slope instability analysis. *Landslides*, *12*(1), 165–175. https://doi.org/10.1007/s10346-014-0536-3

Zong, J., Zhang, C., Liu, L., & Liu, L. (2024). Modeling Rainfall Impact on Slope Stability: Computational Insights into Displacement and Stress Dynamics. *Water*, *16*(4), 554. https://doi.org/10.3390/w16040554